

Fluctuation theorem for constrained equilibrium systems

Thomas Gilbert^{1,*} and J. Robert Dorfman^{2,†}

¹*Center for Nonlinear Phenomena and Complex Systems, Université Libre de Bruxelles,
Code Postal 231, Campus Plaine, B-1050 Brussels, Belgium*

²*Department of Physics and Institute for Physical Science and Technology,
University of Maryland, College Park, Maryland 20742*

(Dated: December 24, 2021)

We discuss the fluctuation properties of equilibrium chaotic systems with constraints such as isokinetic and Nosé-Hoover thermostats. Although the dynamics of these systems does not typically preserve phase-space volumes, the average phase-space contraction rate vanishes, so that the stationary states are smooth. Nevertheless finite-time averages of the phase-space contraction rate have non-trivial fluctuations which we show satisfy a simple version of the Gallavotti-Cohen fluctuation theorem, complementary to the usual fluctuation theorem for non-equilibrium stationary states, and appropriate to constrained equilibrium states. Moreover we show these fluctuations are distributed according to a Gaussian curve for long-enough times. Three different systems are considered here, namely (i) a fluid composed of particles interacting with Lennard-Jones potentials; (ii) a harmonic oscillator with Nosé-Hoover thermostatting; (iii) a simple hyperbolic two-dimensional map.

PACS numbers: 05.70.Ln, 05.40.-a

Recently some papers have appeared which discuss the applicability of the Gallavotti-Cohen Fluctuation Theorem (FT) [1] to near equilibrium and equilibrium chaotic systems subject to isokinetic and Nosé-Hoover thermostats [2, 3, 4]. In particular, in [2], Evans *et al.* consider constrained isokinetic systems of interacting particles which are in equilibrium or near equilibrium states and claim the fluctuations of the phase-space contraction rate of the systems at or near equilibrium do not satisfy the FT.

One of the issues under discussion in these papers is whether or not the FT applies when the external forces vanish, which we refer to as constrained equilibrium. These systems differ from genuine equilibrium ones because of the action of a constraint, for instance acting so as to keep the kinetic energy constant. For systems consisting of particles with instantaneous, elastic, hard ball collisions the total energy is all kinetic and the constraint has no effect in the absence of external forces, thus the resulting ensemble is the usual microcanonical one. For other systems the kinetic and total energies are not the same. The constraint fixes only the kinetic energy and the total energy fluctuates. As a result, the constrained equilibrium ensemble is not microcanonical, but has a different structure, which we explore here.

For the sake of illustration, let us consider a fluid composed of particles with pair-wise, central interactions, placed in a periodic box, and not subjected to external forces. In the absence of other constraints, the microcanonical measure is the invariant one. Now we modify the dynamics by introducing a (time-reversible) frictional force on the particles with the requirement that

the total kinetic energy remain constant in time, see Eqs. (9), (10) and (14) below for a specific example. Because of this constraint, the total energy is not conserved and the Liouville theorem is violated. In such a case the phase-space flow can have non-vanishing divergence (point-wise), even though it vanishes in average. In other words, as long as there is no external driving, the system relaxes to an equilibrium state, different from the one specified by the volume measure, but nevertheless with vanishing average phase-space contraction rate. For Anosov systems or those satisfying the Chaotic Hypothesis, this implies the sum of the Lyapunov exponents is identically zero. This is to say the stationary measure is smooth both with respect to stable and unstable manifolds [4]. Moreover, the existence of a time-reversal symmetry implies that the equilibrium measure must be symmetric under time-reversal operation, *i. e.* a trajectory and its time reverse are equally as probable. This is indeed what one expects from an equilibrium state, whether it verifies Liouville's theorem or not.

The aim of this paper is to provide through some elementary considerations a characterization of the fluctuations of the phase-space contraction rate of such constrained equilibrium systems, which we will subsequently support through numerical studies of specific examples. The outcome indicates that the FT does apply, in agreement with conclusions reached by Gallavotti *et al.* [4].

For non-equilibrium stationary states, the FT [1] is a statement about the asymmetric part of the probability distribution of the phase-space contraction rate. Let $\bar{\sigma} \equiv \langle \sigma \rangle$ denote the non-zero expectation value of the phase-space contraction rate of the non-equilibrium stationary state of a given system and let $\text{Prob}(\sigma_t = p\bar{\sigma})$ denote the probability of observing, during a time interval of length t , a given fluctuation of the partial average of σ equal to $p\bar{\sigma}$, where the amplitude p is a dimensionless number.

*thomas.gilbert@ulb.ac.be

†rdorfman@umd.edu

The FT [1] states that when $\bar{\sigma} > 0$

$$\lim_{t \rightarrow \infty} \frac{1}{t} \ln \frac{\text{Prob}(\sigma_t = p\bar{\sigma})}{\text{Prob}(\sigma_t = -p\bar{\sigma})} = p\bar{\sigma}. \quad (1)$$

As pointed out in [4], the derivation of this result *assumes* $\bar{\sigma} > 0$ and must be reformulated if $\bar{\sigma} = 0$.

For an equilibrium system, finite-time distributions of the phase-space contraction rate are symmetric about zero. Now let σ denote the point-wise divergence of a flow with the properties described above (or equivalently the logarithm of the Jacobian of a time-discrete mapping with similar properties), and let $\text{Prob}(\sigma = a)$ denote the (equilibrium) probability of observing a given value a of σ . For an equilibrium system, the most general FT is the following :

$$\text{Prob}(\sigma = a) = \text{Prob}(\sigma = -a), \quad (2)$$

which holds since the equilibrium distribution is symmetric under time-reversal (this operation changes the sign of σ). Equation (2) is similar to detailed balance for stochastic systems.

For a system whose phase-space volumes are preserved by the evolution, the probabilities in Eq. (2) are non-vanishing only at $a = 0$, so that no fluctuations occur. But this is not necessarily so for constrained equilibrium systems. If so, one can consider the ratio of the two probabilities, equal to unity, and average σ over some time interval without affecting the result. Let σ_t denote the average of σ over a time interval of length t and take the logarithm of the ratio of Eq. (2) applied to σ_t to obtain the expression

$$\lim_{t \rightarrow \infty} \frac{1}{t} \ln \frac{\text{Prob}(\sigma_t = a)}{\text{Prob}(\sigma_t = -a)} = 0, \quad (3)$$

which is a corollary to Eq. (2) and, as remarked in [4], is the natural generalization of the Gallavotti-Cohen FT, here applied to an equilibrium system. The statement of Eq. (3) is weaker than Eq. (2) and not very useful for its own sake since the equilibrium stationary state carries no asymmetric part. Nevertheless it is correct and not in contradiction with the FT as stated in [1].

This observation does not support the comments by Evans *et al.* [2] that for Anosov equilibrium dynamics the range of the admissible fluctuations for the FT shrinks to zero. While it is true that the asymptotic range of admissible fluctuations of σ_t may shrink to zero as $t \rightarrow \infty$, one should still expect to measure fluctuations about the value $a = 0$ as long as $t < \infty$. Moreover the rate at which $\text{Prob}(\sigma_t = a)$ goes to zero is the same as that of $\text{Prob}(\sigma_t = -a)$, so that the ratio of the two remains constant as $t \rightarrow \infty$. Of course, the right hand side of Eq. (3) being zero, the result is trivial, irrespective of the asymptotic form of the probability distribution. In other words, unlike Eq. (1) for non-equilibrium stationary states, neither Eq. (2), nor Eq. (3) hold any information on the asymptotic form of the probability distribution

of the phase-space contraction rate; the only information provided by Eq. (2) is that the probability distributions are symmetric about their average value, zero. Moreover, Eq. (2) holds for equilibrium systems irrespective of the details of the dynamics, whether it verifies the Chaotic Hypothesis or not. The details of the fluctuations may indeed vary from one system to another, but even though, whether the fluctuations are trivial or not, Eq. (3) always holds.

Here we will show, through the example of an equilibrium hyperbolic map [10] with non-trivial Jacobian, that the distribution of the phase-space contraction rate is symmetric about zero, with an asymptotic form given by $\text{Prob}(\sigma_t = x) \approx \rho_t(x)dx$, with

$$\rho_t(x) = \frac{t}{\sqrt{2\pi\chi^2}} \exp \left[-\frac{(xt)^2}{2\chi^2} \right], \quad (4)$$

where χ is a constant which depends on the specific system under consideration. We note that this indicates that the distribution of the total phase space contraction accumulated in time has a variance that is asymptotically independent of time.

We will show through two additional examples that for both Nosé-Hoover thermostatted equilibrium systems (whose kinetic energy distribution is given by the canonical ensemble distribution) and constrained, equilibrium interacting particle systems, such as a Lennard-Jones fluid with isokinetic thermostat, the asymptotic form of the phase-space contraction rate distribution function is (i) non-trivial, (ii) consistent with the relevant Equilibrium Fluctuation Relations, Eqs. (2-3) and (iii) verifies a central limit theorem similar to Eq. (4), albeit with a time-dependence in \sqrt{t} instead of t .

The first example we consider is a mapping of the unit square into itself with hyperbolic properties similar to the baker map. It is a variant of a non-linear baker map previously introduced by us [5]. Namely let M_a be defined by

$$M_a(x, y) = \begin{cases} (2\varphi_a(x), \varphi_{-a}(y/2)), & 0 \leq x < 1/2, \\ (2\varphi_a(x) - 1, \varphi_{-a}((y+1)/2)), & 1/2 \leq x < 1, \end{cases} \quad (5)$$

where

$$\varphi_a(x) = \begin{cases} (1/\pi) \arctan [\tan(\pi x)2^{-a}], & 0 \leq x < 1/2, \\ 1 + (1/\pi) \arctan [\tan(\pi x)2^{-a}], & 1/2 \leq x < 1. \end{cases} \quad (6)$$

The time-reversibility of M_a under the time-reversal operator $T(x, y) = (1 - y, 1 - x)$ is easy to check. Moreover, as long as $0 \leq a < 1$, M_a is uniformly expanding along the x -coordinate, while it is contracting along the y -coordinate. It is smooth, *i. e.* it is continuous and has continuous derivative everywhere, but for the cut at $x = 1/2$. Therefore it shares the hyperbolic properties of the usual baker map. The Jacobian, which we denote $|DM_a(x, y)|$, is typically not equal to unity, but the

natural invariant measure of this map turns out to be absolutely continuous, as far as one can tell from numerical simulations. This is illustrated in Fig. 1 where the parameter was set to $a = 1/2$. The symmetry of the invariant measure under the time-reversal operator is clearly seen from the figure.

The smoothness of the invariant measure is consistent with the computation of the Lyapunov exponents, which, for this value of the parameter, are numerically found to be $\lambda_+ = 0.6472 + o(10^{-4})$, $\lambda_- = -0.6472 + o(10^{-4})$, *i. e.* within numerical errors $\lambda_+ + \lambda_- = 0$. Figure 2 shows a numerical computation of the probability distribution function of the logarithm of the Jacobian of M_a , which is symmetric about 0, as expected from Eq. (2). The probability distributions of the time-averaged Jacobian are shown in Fig. 3-4.

The second example we consider is that of a harmonic oscillator with a so-called Nosé-Hoover chain of thermostats here limited to two thermostat variables. This generalization of the Nosé-Hoover thermostating scheme is due to [6]. The system is time-reversible and yields canonical distributions of the phase variables, as shown in [7].

Let q denote the position variable, p the momentum, ζ and ξ the thermostating variables. Taking all the oscillator parameters to be unity, the equations of motion are (see p. 193 of [7])

$$\begin{aligned}\dot{q} &= p, \\ \dot{p} &= -q - \zeta p, \\ \dot{\zeta} &= p^2 - 1 - \xi \zeta, \\ \dot{\xi} &= \zeta^2 - 1.\end{aligned}\tag{7}$$

In the absence of a thermostating mechanism, oscillations would be periodic of period 2π , but this is no longer so if the thermostating mechanism is turned on.

The phase-space contraction rate is $\sigma = -\zeta - \xi$ whose distribution, computed numerically with an adaptive step size 5th order Runge-Kutta scheme [8], is shown in Fig. 5. This curve is Gaussian with standard deviation $\sqrt{2}$, consistent with the analytical result given in [7], p. 193. Distributions of time-averaged contraction rates σ_t are shown in Figs. 6-7. Deviations from an exact Gaussian can be seen for intermediate times, which are due to surviving correlations. However, these deviations disappear for long enough times, so that one retrieves a Gaussian distribution whose asymptotic form is now given by $\text{Prob}(\sigma_t = x) \approx \rho_t(x)dx$, with

$$\rho_t(x) = \sqrt{\frac{t}{2\pi\chi^2}} \exp\left[-\frac{(x)^2 t}{2\chi^2}\right].\tag{8}$$

Notice the time dependence is different from Eq. (4).

The third example we consider is that of a Lennard-Jones fluid with the kinetic energy constrained to a constant value,

$$\dot{\mathbf{q}}_i = \mathbf{p}_i,\tag{9}$$

$$\dot{\mathbf{p}}_i = \sum_{j \neq i} \mathbf{F}(q_{ij}) - \alpha \mathbf{p}_i,\tag{10}$$

where $\mathbf{F}(q_{ij})$ denotes the force between particles i and j associated to the usual Lennard-Jones potential, and q_{ij} is the distance separating the particles,

$$\mathbf{F}(r) = -\nabla\phi(r),\tag{11}$$

$$\phi(r) = 4\epsilon \left[\left(\frac{r}{\sigma}\right)^{12} - \left(\frac{r}{\sigma}\right)^6 \right],\tag{12}$$

$$q_{ij} = |\mathbf{q}_i - \mathbf{q}_j|.\tag{13}$$

The damping term α in Eq. (10) is a function of the phase-space coordinates, derived from the condition that the kinetic energy be constant and such that the equations (9-10) are time-reversal symmetric,

$$\alpha = \frac{\sum_{i,j \neq i} \mathbf{p}_i \cdot \mathbf{F}(q_{ij})}{\sum_i p_i^2}.\tag{14}$$

One readily sees α is precisely minus the divergence of the flow (up to a multiplicative constant), and therefore the quantity whose probability distribution is expected to be symmetric about zero according to Eq. (2). This has been checked numerically for a two-dimensional fluid of 8 particles in a box of approximately 7×8 units of length squared, using the modified Verlet leapfrog algorithm, as described in [9].

The resulting probability distribution of α is shown in Fig. 8 and the probability distributions of its time average in Figs. 9-10.

In summary, we have shown for three examples of constrained equilibrium chaotic systems, that the probability distributions of the phase-space contraction are symmetric about zero and verify a central limit theorem. The time-dependence varies according to the nature of the dynamics. It would be interesting to further investigate this property.

Acknowledgments

The authors thank G. Gallavotti and P. Gaspard, as well as D. Evans and L. Rondoni for their comments on this work. TG is chargé de recherches with the F. N. R. S. (Belgium). JRD acknowledges support from the National Science Foundation (USA) under Grant PHY 01-38697.

[1] G. Gallavotti and E. G. D. Cohen, Phys. Rev. Lett. **74** 2694 (1995); J. Stat. Phys. **80** 931 (1995).

[2] D. J. Evans, D. J. Searles, and L. Rondoni, Phys. Rev. E **71** 056120 (2005).

- [3] M. Dolowschiak and Z. Kovacs, Phys. Rev. E **71**, 025202(R), (2005).
- [4] F. Bonetto, G. Gallavotti, A. Giuliani, and F. Zamponi, *Chaotic hypothesis, fluctuation theorem and singularities*, cond-mat/0507672.
- [5] T. Gilbert, C. D. Ferguson, and J. R. Dorfman, Phys. Rev. E **59**, 364, (1999).
- [6] G. J. Martyna, M. L. Klein, and M. Tuckerman, J. Chem. Phys. **97** 2635 (1992)
- [7] W. G. Hoover, *Time reversibility, computer simulation, and Chaos*, (World Scientific, Singapore, 1999).
- [8] William H. Press, Brian P. Flannery, Saul A. Teukolsky, William T. Vetterling, *Numerical Recipes in Fortran*, Second edition (Cambridge University Press, Cambridge, 1992).
- [9] D. Brown and J. H. R. Clarke, Molecular Phys. **51** 1243 (1984).
- [10] Unlike Anosov systems, which are assumed to be continuously hyperbolic, we will allow for discontinuities in the hyperbolicity, much like with the finite horizon periodic Lorentz Gas or with the baker map.

Figures

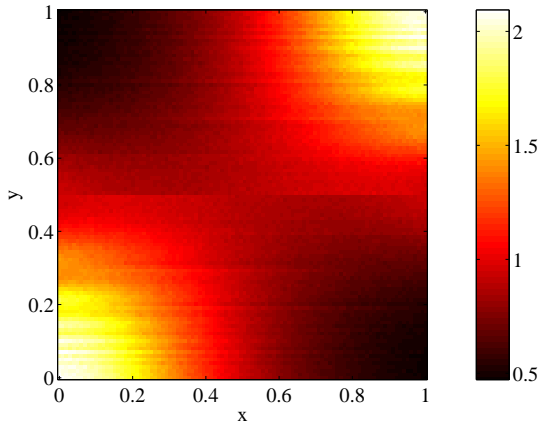


FIG. 1: (Color online) Numerical computation of the invariant density of $M_a(x, y)$ Eq. (5) for $a = 1/2$. The computation is the result of 10^4 trajectories iterated over a time of 10^3 steps. The same time was discarded prior to outputting trajectories in order to eliminate transient effects.

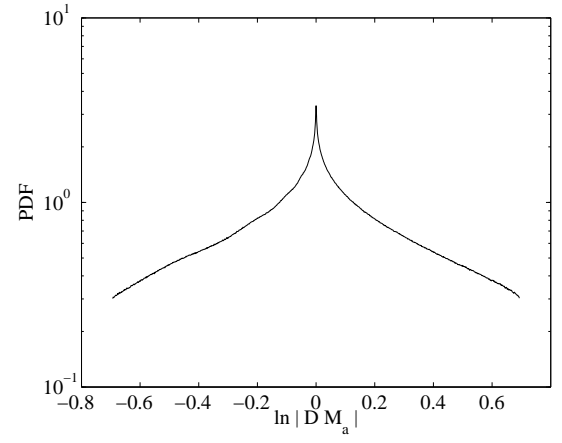


FIG. 2: Numerical computation of the probability density of the logarithm of the Jacobian of $M_a(x, y)$ Eq. (5) for $a = 1/2$. The computation is the result of sampling 10^4 trajectories iterated over a time of 10^4 steps. 10^3 bins were used.

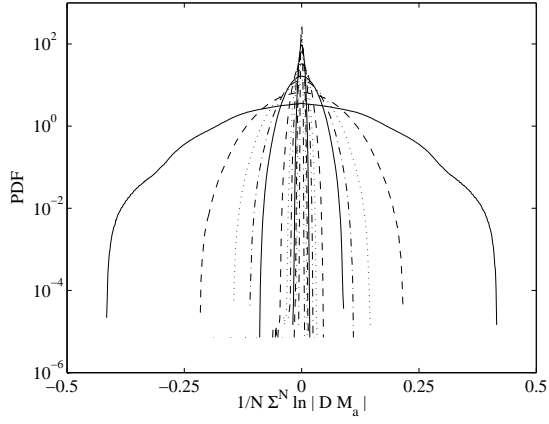


FIG. 3: Numerical computation of the probability density of the logarithm of the time-averaged Jacobian of $M_a(x, y)$ Eq. (5) for $a = 1/2$. The curves shown here are averaged respectively over $N = 5, 10, 15, 20, 25, 50, 75, 100, 150, 200, 250$, and 500 steps (the curves get narrower as the number of steps increases). The computation is the result of sampling 10^4 trajectories iterated over a time of 10^4 steps. 10^3 bins were used.

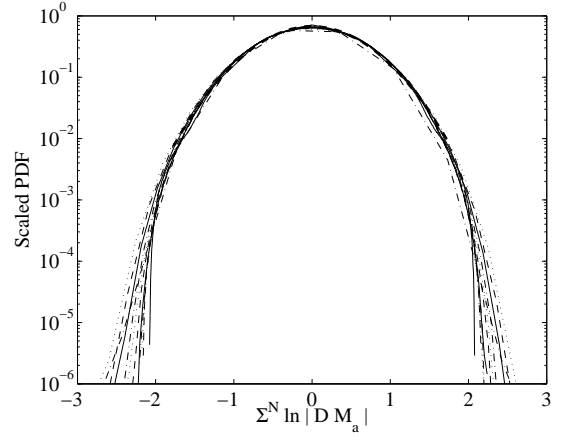


FIG. 4: Same as Fig. 3 with the curves rescaled according to Eq. (4). The thick dashed curved is a Gaussian with standard deviation $\chi^2 = 0.35$.

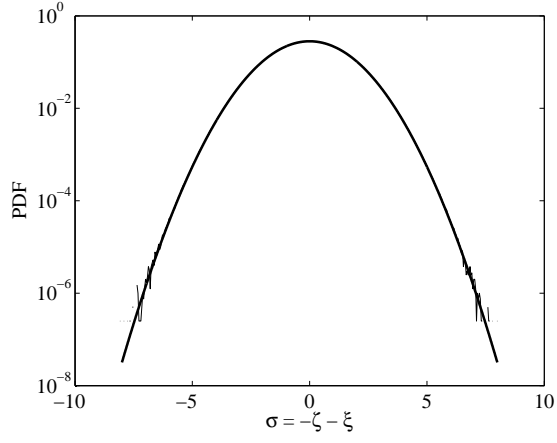


FIG. 5: Numerical computation of the probability density of $-\zeta - \xi$, the divergence of the Nosé-Hoover oscillator, Eq. (7), for the trajectory with initial conditions are $q_0 = 0$, $p_0 = 1$, $\zeta_0 = 0.5$, $\xi_0 = 0$. The integration is performed over a time $2\pi \times 10^8$, sampled every 2π , with 500 bins spanning $[-10, 10]$. The thick line on top is a Gaussian with standard deviation $\sqrt{2}$.

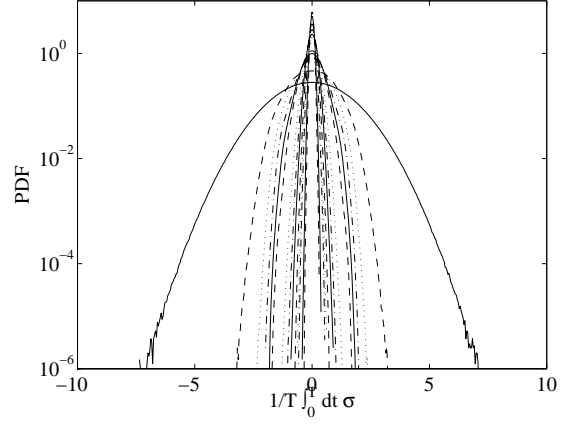


FIG. 6: Numerical computation of the probability density of the time-averaged contraction rate σ_t , for times $T = 1, 5, 10, 15, 20, 25, 50, 75, 100, 150, 200, 250, 500$ and 750 (times 2π). The parameters of the integration are the same as Fig. 5.

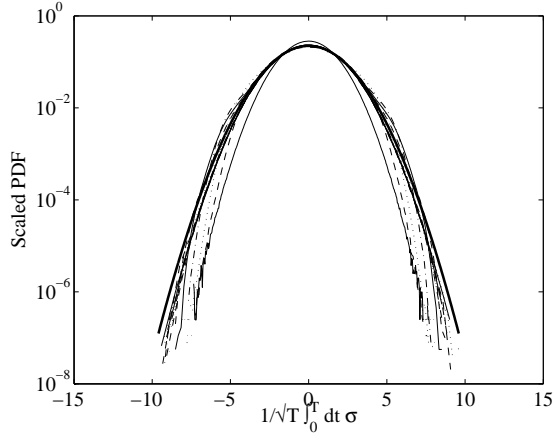


FIG. 7: Same as Fig. 6 with the curves rescaled according to Eq. (8). The thick curve is a Gaussian with standard deviation $\chi^2 = 3.2$. The agreement is excellent for times 200 and greater.

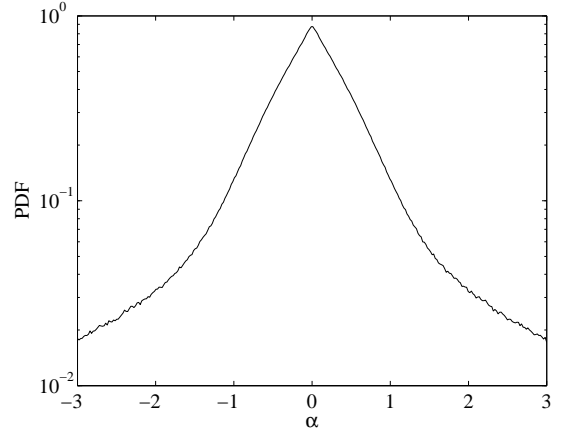


FIG. 8: Numerical computation of the probability distribution of α , the damping term in Eq. (10). The parameters of the simulation correspond to the usual choice of dimensionless parameters. 8 particles were used on a periodic 2-dimensional box of size approximately 7×8 . The temperature was set to $T = 1$ and the particle masses to $m = 1$. A number of 10^4 trajectories were taken and the value of α recorded for 1000 units of time at intervals of 1 time units. 300 bins were used, spanning values $\alpha \in [-3, 3]$. The average value of α was computed to be $\approx 2.7 \times 10^{-4}$ with standard deviation $\approx 1.8 \times 10^{-3}$. About 8.7% of the computed values fell out of the range shown in the figure.

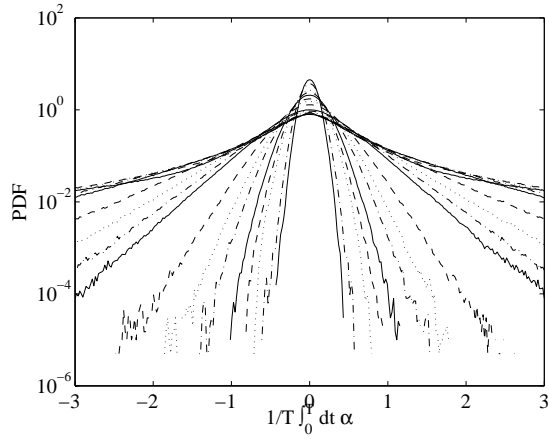


FIG. 9: Same as Fig. 8 for the time-average $\alpha_t = 1/T \int_0^T \alpha$, for times $T = 1, 2, 3, 4, 5, 10, 15, 20, 25, 50, 75, 100, 150, 200, 250, 500$ and 750 .

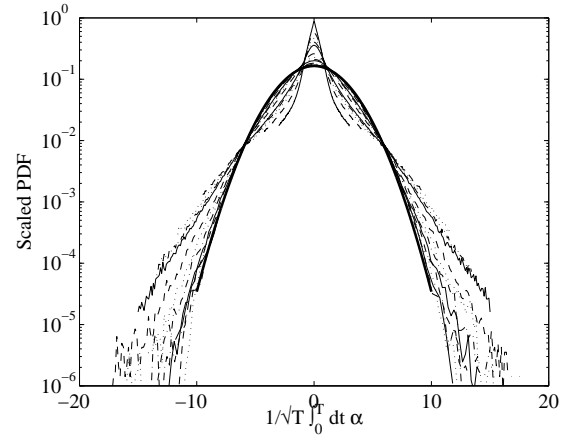


FIG. 10: Same as Fig. 9 with the curves rescaled according to Eq. (8). The thick curve is a Gaussian with standard deviation $\chi^2 = 5.9$. The agreement is excellent for times 200 and greater.